

# A Study of Deformation-Produced Deep Levels in *n*-GaAs Using Deep Level Transient Capacitance Spectroscopy

T. Ishida\*, K. Maeda, and S. Takeuchi

The Institute for Solid State Physics, The University of Tokyo,  
Minato-ku, Tokyo 106, Japan

Received 23 August 1979/Accepted 1 November 1979

**Abstract.** Deformation-produced deep levels, both of electron and hole traps, have been studied using deep level transient capacitance spectroscopy (DLTS) for an undoped *n*-type GaAs (HB grown) compressed at 440 °C. Concentrations of two grown-in electron trap levels ( $E_c - 0.65$  eV and  $E_c - 0.74$  eV) and one grown-in hole trap level ( $E_v + \sim 0.4$  eV) increase with plastic deformation, while that of a grown-in electron trap level ( $E_c - \sim 0.3$  eV) decreases in an early stage of deformation. While no new peak appeared in the electron trap DLTS spectrum after plastic deformation, in the hole trap DLTS spectrum a broad spectrum, seemingly composed of many peaks, newly appeared in a middle temperature range, which may be attributed to electronic energy levels of dislocations with various characters.

**PACS:** 61.70, 71.55

In recent years deep levels associated with intrinsic lattice defects as well as extrinsic defects in semiconducting materials have been extensively studied by use of deep level transient capacitance spectroscopy (DLTS) as a powerful tool [1]. As for GaAs, various levels in the forbidden energy gap, both of the electron trap and the hole trap, have been reported to be produced by irradiation of high energy particles [2]. On the other hand, no such experiments have been reported for deformation-produced lattice defects, except for a recent paper on Si [3]. Especially, electronic energy levels at the core of dislocations in semiconducting materials have long received considerable interest because of its high electronic activity. Although various techniques have been applied to obtain dislocation levels (for GaAs resistivity and photoconductivity measurements have recently been applied to this end [4, 5]), there still remain ambiguities in the interpretation of the results, e.g. which carriers, electrons or holes, take part in the transitions involved in the measurements. The capacitance DLTS can discriminate the participating carrier type by the sign of the

capacitance change. This technique has also an advantage of its high sensitivity, which is suitable for the measurement of small amount of defects such as those introduced by plastic deformation. In this report, we present changes of the DLTS spectra, both of the electron trap and the hole trap, with plastic deformation of *n*-type GaAs.

## 1. Experimental Procedures

An undoped *n*-type GaAs (grown by the horizontal Bridgman method) purchased from Sumitomo Electric Industries, Ltd. was used; carrier concentration being  $10^{16}$  cm<sup>-3</sup> and the initial etch pit density less than  $10^4$  cm<sup>-2</sup>. The crystal was cut into rectangular specimens with dimensions and orientation show in Fig. 1. This orientation was chosen because it ensures the single slip deformation and also allows us to measure the dislocation density on the side surface. After chemically polished, the specimen was sandwiched by high-purity alumina single crystal plates, and was compressed in a molybdenum compression jig along the  $[\bar{1}23]$  axis to various amount of strain at 440 °C in a purified argon atmosphere at a strain-rate of  $\sim 1 \times 10^{-4}$  s<sup>-1</sup>. To check the possible specimen con-

\* Present address: Nippon Kogaku Co., Ltd., Nishi-Ohi, Shinagawa-ku, Tokyo 140, Japan

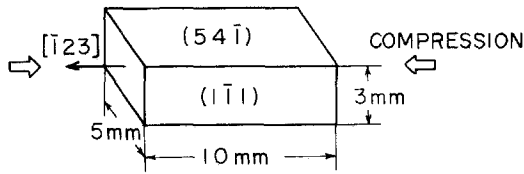


Fig. 1. Orientation and size of compression specimens

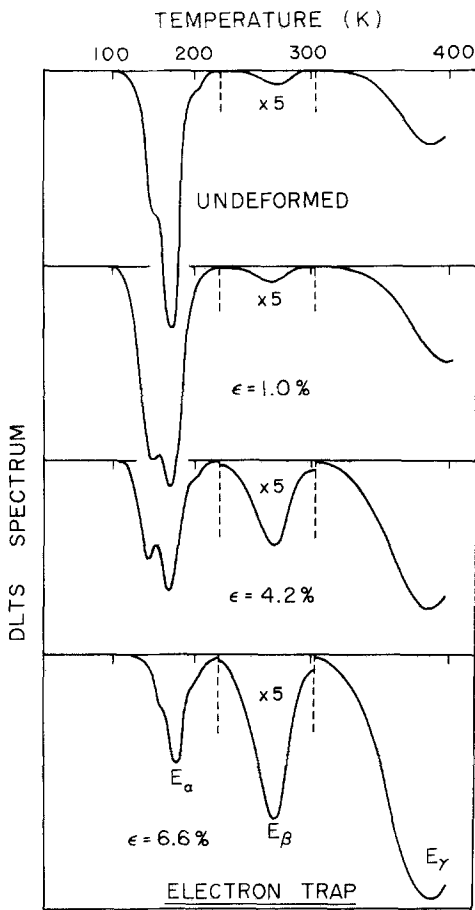


Fig. 2. Examples of electron trap DLTS spectra with rate windows at 1.95 ms and 7.80 ms for undeformed and deformed specimens

tamination during the high temperature test, a control sample was always placed near the compression specimen on the alumina plate. After unloaded, the specimen was cooled down to 100 °C within 30 min. Etch-pit density after deformation was counted using a scanning electron microscope on the etched (111) surface.

For convenience of the experimental set-up for DLTS measurements and to take three samples from a deformed specimen, each specimen was cut and polished into slices of about 1 mm thickness parallel to the (541) plane. An ohmic contact film was deposited on one

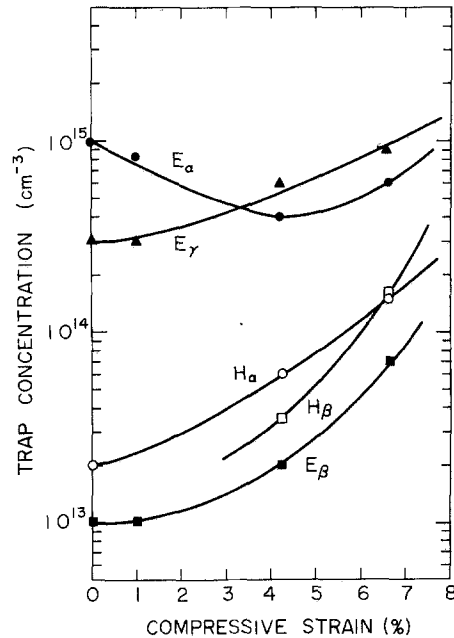


Fig. 3. Trap concentrations of three electron traps and two hole traps as a function of compressive strain

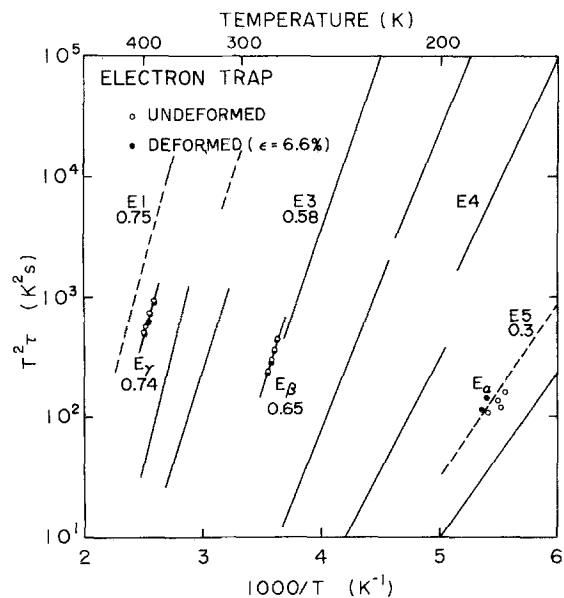


Fig. 4.  $T^2\tau - 1/T$  plots for three electron trap levels,  $E_\alpha$ ,  $E_\beta$  and  $E_\gamma$ , of an undeformed sample and a deformed one ( $\epsilon = 6.6\%$ ). Other lines which are obtained by other workers have been taken from a review paper by Ikoma et al. [10]. Dashed portions of the lines are extrapolated ones. Numerals indicate activation energies in eV

side of the sample by evaporating a Au-Sn (10 : 1) alloy followed by diffusion annealing at 440 °C for 2 min in a purified  $H_2$  atmosphere, and on the other side a Schottky contact film of gold was evaporated. The DLTS measurement of majority carrier traps, or electron traps in our case, was carried out using a system

Table 1. Energy levels and cross sections of three electron traps and two hole traps

Trap	Energy level [eV]	Cross section [cm <sup>2</sup> ]
$E_x$	$E_c - 0.3$	$\sim 1 \times 10^{-14}$
$E_\beta$	$E_c - 0.65$	$5 \sim 8 \times 10^{-12}$
$E_\gamma$	$E_c - 0.74$	$2 \sim 3 \times 10^{-13}$
$H_x$	$E_v + 0.4$	$\sim 10^{-14}$
$H_\beta$	$E_v + 0.46$	$\sim 10^{-16}$

composed of an injection pulse generator, a capacitance meter (Boonton 72B), a sample and hold circuit, a differential amplifier, a signal averager and an  $X - Y$  recorder. The response time of the system was 1 ms. A positive injection pulse of 1 ms in every 10 ms was applied to the sample negatively biased by 3 V. The temperature scan was done between 120 K and 400 K.

The measurement of minority carrier traps, or hole traps, was performed using an optical DLTS method [6]. A light with the wave length around the intrinsic absorption (800 ~ 1200 nm) through a monochromator from a halogen lamp (150 W) was mechanically chopped (100 c/s) and was illuminated on the sample to inject carriers in duration of 1 ms. Using a trigger delay circuit and the same capacitance transient measurement system as in the majority carrier trap measurement, the hole trap DLTS signal of samples reversely biased by 2 V was recorded on the  $X - Y$  recorder. More than one sliced samples were measured for each deformed specimen. Reproducibility of the spectrum was good except at lower temperature than 200 K.

## 2. Results

By comparing control samples and unannealed samples, it was confirmed that no appreciable change in the DLTS spectra, both of the electron and the hole traps, took place after the high temperature treatment of the deformation experiment, and thus any changes in the DLTS spectra with plastic deformation are due to deformation-produced lattice defects.

Figure 2 shows examples of the DLTS spectra for electron traps obtained using rate windows at 1.95 ms and 7.80 ms. Three distinct peaks,  $E_x$ ,  $E_\beta$  and  $E_\gamma$ , are seen in the undeformed crystal. As the plastic strain increases, the relative heights of these peaks change but no new peak appears. Concentrations of these traps estimated from the extrapolated capacitance,  $\Delta C(t=0)$ , are shown in Fig. 3 as a function of the compressive strain. To obtain activation energies and capture cross sections of these levels, the standard  $T^2\tau - 1/T$  plots [7] have been done. An example of

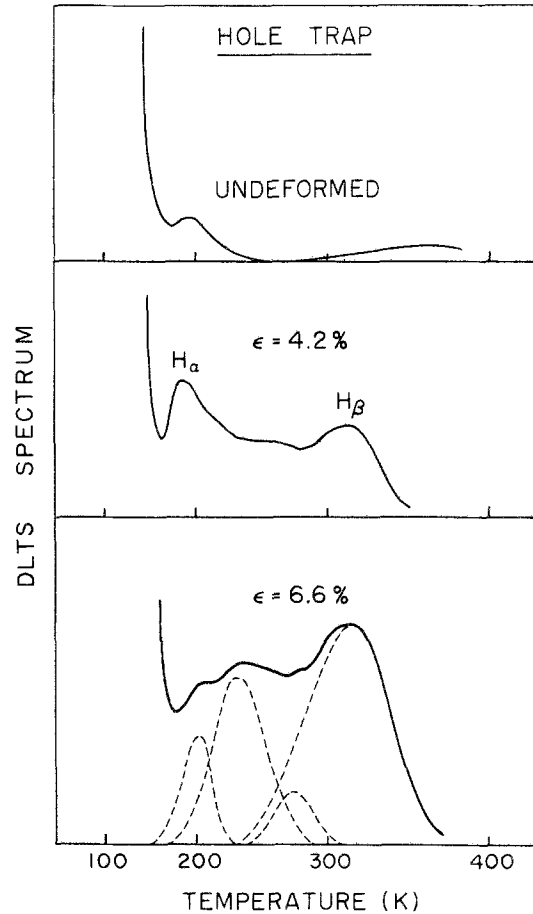


Fig. 5. Hole trap DLTS spectra with rate windows at 1.95 ms and 7.80 ms for undeformed and deformed specimens

such plots is given in Fig. 4 for a deformed sample ( $\epsilon = 6.6\%$ ) and an undeformed control sample. The activation energy of each trap, which corresponds to the depth of the energy level from the conduction band, was determined by averaging the slopes of the corresponding trap of all the samples and is tabulated in Table 1. The capture cross section obtained on the assumption of the temperature independent cross section is also given in Table 1.

In the DLTS spectrum for minority carrier traps of the undeformed specimen, three peaks can be seen as shown in the upper spectrum of Fig. 5; a large peak at  $\sim 150$  K of which entire shape could not be recorded, a small peak at  $\sim 200$  K labeled  $H_x$ , and a broad, low peak at high temperature which disappeared after deformation. On the other hand, in deformed specimens a continuous, broad peak appeared in the middle temperature range as seen in Fig. 5. This broad peak seems to consist of many peaks such as those shown by dotted lines in the lower spectrum in Fig. 5; among them the highest temperature peak of  $H_\beta$  is the most distinct. The estimated concentrations of  $H_x$  and  $H_\beta$

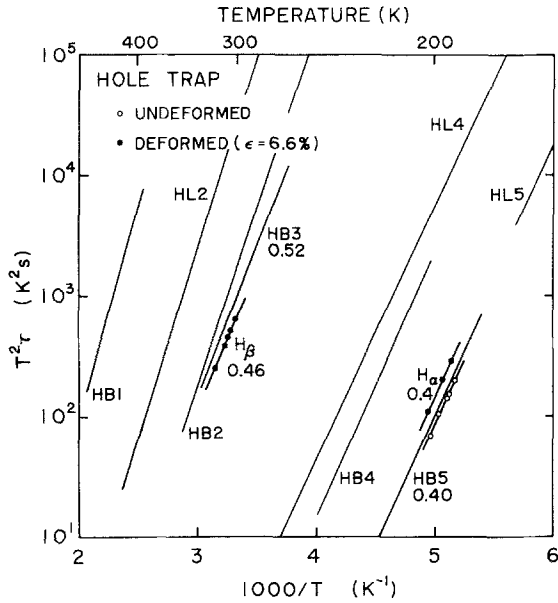


Fig. 6.  $T^2\tau - 1/T$  plots for two hole trap levels,  $H_\alpha$  and  $H_\beta$ . Other lines have been taken from a paper by Mitonneau et al. [15]

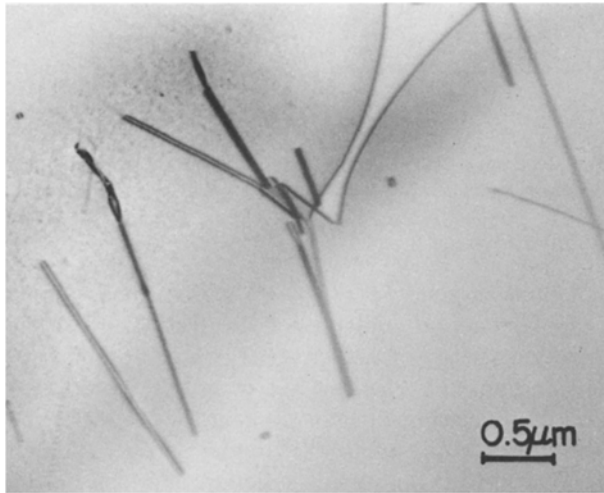


Fig. 7. Electron micrograph of a specimen compressed by 1.4% at 440°C showing that most dislocations form dipoles. Foils were taken parallel to the primary (111) slip plane

traps are plotted also in Fig. 3 as a function of the plastic strain. Figure 6 shows an example of  $T^2\tau - 1/T$  plots for hole traps. The analyzed activation energies and the cross sections for the above two traps are also given in Table 1.

Etch-pit densities counted were  $2 \sim 3 \times 10^7 \text{ cm}^{-2}$  and  $5 \sim 7 \times 10^7 \text{ cm}^{-2}$  for specimens deformed by 4.2% and 6.6%, respectively. The dislocation distribution was fairly uniform in these specimens.

### 3. Discussion

If we consider a dislocation line as an array of trapping centers separated by an atomic distance  $a$ , then the concentration of the center in a crystal with a dislocation density  $\rho$  is  $\rho/a$ . In the undeformed crystals used in the present investigation, the grown-in dislocation density was so low ( $\lesssim 10^4 \text{ cm}^{-2}$ ) that the trapping center associated with dislocations should not be detected because of negligible concentration ( $\sim 10^{11} \text{ cm}^{-3}$ ). In other words, no centers detected in the undeformed crystal, whether or not they change their concentrations with plastic deformation, are of dislocation origin.

In the present DLTS spectra, no electron trap level associated with deformation-produced dislocations were detected. This is consistent with the recent result of the scanning DLTS measurement by Lang et al. on  $\text{Al}_x\text{Ga}_{1-x}\text{As}$  [8], where in the spatially localized positive DLTS signal from dark line defects, which have been verified to correspond to dislocation networks [9], no particular peak other than that observed in the outside region is observed. Comparing  $T^2\tau - 1/T$  plots of the three electron traps,  $E_\alpha$ ,  $E_\beta$  and  $E_\gamma$ , with other DLTS measurements compiled by Ikoma et al. [10], as shown in Fig. 4, it is found that any of these levels nearly coincide with some of the electron traps observed by other investigators in as-grown or irradiated GaAs crystals although some discrepancies in the activation energy were seen. The  $E_\gamma$  level seems to correspond to the level E1 labeled by Ikoma et al. [10], which has been observed commonly in GaAs crystals grown by various methods; Czochralsky (Cz), horizontal Bridgman (HB) and vapor phase epitaxial (VPE) methods. This level has been ascribed to oxygen [11] or to gallium vacancy [12], but recently it was concluded that oxygen is not involved in this level [13]. The present result supports the native origin because the concentration of the  $E_\gamma$  level changed only by deformation. The  $E_\beta$  level appears to correspond to the trap B obtained in VPE wafers by Mircea and Mitonneau [14] (labeled E3 in [10]), though the activation energies are considerably different. The plots of the  $E_\gamma$  level are largely scattered but located around the E5 level detected in HB wafers [10]. The physical origins of the latter two levels are not known.

It is well-known that the plastic deformation produces not only dislocations but also point defects due to dragging jogs on screw dislocations formed by the dislocation intersection or the cross slip. Also, glide dislocations can absorb point defects already present on the slip plane. As seen in Fig. 3, the electron trap  $E_\beta$  and  $E_\gamma$  increased their concentrations with increasing deformation while the change of  $E_\alpha$  trap was not

monotonic. Considering that increase or decrease of concentration of point defects depends on the relative rates of the production and the absorption, it is no wonder that defects behave differently according to their nature.

Comparison in the  $T^2\tau-1/T$  plots is given in Fig. 6 between hole traps of  $H_\alpha$  and  $H_\beta$  and hole traps observed by other investigators compiled by Mitonneau et al. [15]. The hole trap  $H_\alpha$ , which exists in the as-grown crystal and increases its concentration with deformation, is found to correspond to the hole trap labeled HB5 and HL5. This hole trap has been observed always in undoped LPE grown crystals [7] and could be attributed to some kind of native point defect.

On the other hand, the hole trap  $H_\beta$ , which was not detected in the undeformed control sample, was found to correspond to no reported hole traps of native origin except of chemical origin of Fe labeled HB3 in Fig. 6 [15]. Thus, this level is possibly due to dislocations. From the etch pit density, the concentration of dislocation level in the sample deformed by 6.6% is estimated to be of the order of  $10^{15} \text{ cm}^{-3}$ , which can account for the observed trap concentration in Fig. 3. The energy level of  $H_\beta$  ( $E_v + 0.46 \text{ eV}$ ) almost coincides with one of the two dislocation levels ( $E_c - 0.9 \text{ eV}$  and  $E_c - 0.7 \text{ eV}$ ) obtained by Nakata [5]. However, the hole capture cross section of the dislocation is, though not known exactly how big it is, usually conjectured to be larger than those of ordinary point defects from the theory [16] and from the fact that dislocations play an important role as effective killers in degraded optoelectronic devices [9]. In fact, recent measurements of carrier capture cross section in deformed Si [3] gave the largest cross section for dislocation-ascribed traps (labeled  $E(0.38)$ ,  $H(0.35)$  in [3]) among all the traps observed. The obtained value of the cross section for the trap  $H_\beta$  in Table 1 seems too small for dislocations; therefore, the above assignment of  $H_\beta$  is yet tentative.

The other hole trap peaks between  $H_\alpha$  and  $H_\beta$ , which grew up with deformation, overlap each other and physical quantities of these traps could not be de-

termined. Deformed crystals contain various types of dislocations, the  $\alpha$ -dislocation, the  $\beta$ -dislocation and the screw dislocation; these are expected to have different energy levels. Transmission electron microscope observation of thin foils parallel to the primary slip plane of a deformed specimen have shown that majority of dislocations form dipoles as shown in Fig. 7; that is, the two component of edge dislocations,  $\alpha$ - and  $\beta$ -dislocations, are paired. Taking account of these facts, wide spectrum between  $H_\alpha$  and  $H_\beta$  is likely to correspond to various dislocation types. To examine each type of dislocation separately, it is essential to introduce each type of dislocation separately in a specimen, e.g. by careful bending deformation.

*Acknowledgements.* The authors would like to express their hearty thanks to Prof. T. Ikoma of the Institute of Industrial Science, The University of Tokyo, for kind guidance throughout the present work. They also thank M. Ogura for his help in sample preparation and DLTS measurements.

## References

1. D.V.Lang: J. Appl. Phys. **45**, 3023–3032 (1974)
2. D.V.Lang: In *Radiation Effects in Semiconductors 1976*, ed. by N.B.Urli and J.W.Corbett (The Institute of Physics, Bristol 1977) pp. 70–94
3. L.C.Kimerling, J.R.Patel: Appl. Phys. Lett. **34**, 73–75 (1979)
4. H.Nakata, T.Ninomiya: J. Phys. Soc. Jpn. **42**, 552–558 (1977)
5. H.Nakata: Doctoral Thesis, University of Tokyo (1979)
6. A.Mitonneau, G.M.Martin, A.Mircea: In *Gallium Arsenide and Related Compounds* (Edinburgh), 1976, ed. by C. Hilsum (The Institute of Physics, Bristol 1977) pp. 73–83
7. D.V.Lang, R.A.Logan: J. Electron. Mater. **4**, 1053–1066 (1975)
8. D.V.Lang, P.M.Petroff, R.A.Logan, W.D.Johnston, Jr.: Phys. Rev. Lett. **42**, 1353–1356 (1979)
9. P.M.Petroff, R.L.Harman: J. Appl. Phys. **45**, 3899–3903 (1974)
10. T.Ikoma, M.Takikawa, T.Okumura: Proc. 8th Internat. Conf. on Solid State Devices, Japan. J. Appl. Phys. Suppl. **16-1**, 233–232 (1977)
11. R.Williams: J. Appl. Phys. **37**, 3411–3416 (1966)
12. F.Hasegawa, A.Majerfeld: Electron. Lett. **12**, 52–53 (1976)
13. A.M.Huber, N.T.Linh, M.Valladon, J.L.Debrun, G.M.Martin, A.Mitonneau, A.Mircea: J. Appl. Phys. **50**, 4022–4026 (1979)
14. A.Mircea, A.Mitonneau: Appl. Phys. **8**, 15–21 (1975)
15. A.Mitonneau, G.M.Martin, A.Mircea: Electron. Lett. **13**, 666–668 (1977)
16. R.A.Vardanyan: Sov. Phys. JETP **46**, 1210–1213 (1977)